Biogeosciences Discuss., 10, 1605–1634, 2013
www.biogeosciences-discuss.net/10/1605/2013/
doi:10.5194/bgd-10-1605-2013

Biogeosciences
Discussions
Open Access

Multiyear precipitation reduction strongly decrease carbon uptake over North China

W. P. Yuan[1], D. Liu[1], W. J. Dong[1], S. G. Liu[2], G. S. Zhou[3,4], G. R. Yu[5], T. B. Zhao[6], J. M. Feng[1,6], Z. G. Ma[6], J. Q. Chen[7], Y. Chen[1], S. P. Chen[4], S. J. Han[8], J. P. Huang[9], L. H. Li[4], H. Z. Liu[10], S. M. Liu[11], M. G. Ma[12], Y. F. Wang[13], J. Z. Xia[1], W. F. Xu[1], Q. Zhang[14], X. Q. Zhao[15], and L. Zhao[15]

[1]State Key Laboratory of Earth Surface Processes and Resource Ecology, College of Global Change and Earth System Science, Beijing Normal University, Beijing 100875, China
[2]United States Geological Survey, Earth Resources Observation and Science Center, Sioux Falls, South Dakota 57198, USA
[3]Chinese Academy of Meteorological Sciences, Beijing 100081, China
[4]State Key Laboratory of Vegetation and Environmental Change, Institute of Botany, The Chinese Academy of Sciences, Beijing 100093, China
[5]Institute of Geographic Sciences and Natural Resources Research, Chinese Academy of Sciences, Beijing, 100101, China
[6]Key Laboratory of Regional Climate, Environment Research for Temperate East Asia, Institute of Atmospheric Physics, Chinese Academy of Sciences, Beijing 100029, China
[7]Department of Environmental Sciences, University of Toledo, Toledo, OH 43606, USA
[8]Institute of Applied Ecology, Chinese Academy of Sciences, Shenyang 110016, China
[9]Lanzhou University, Lanzhou, Gansu 730000, China

[10]Institute of Atmospheric Physics, Chinese Academy of Sciences, Beijing 100029, China
[11]School of Geography, Beijing Normal University, Beijing 100875, China
[12]Cold and Arid Regions Environmental and Engineering Research Institute, Chinese Academy of Sciences, Lanzhou, Gansu 730000, China
[13]College of Life Sciences, University of Chinese Academy of Sciences, Beijing 100049, China
[14]Meteorological Bureau of Gansu Province, Lanzhou, Gansu 730000, China
[15]Key Laboratory of Qinghai-Tibetan Plateau Biological Evolution and Adaptation, Northwest Institute of Plateau Biology, The Chinese Academy of Sciences, Xining, Qinghai, China

Received: 11 January 2013 – Accepted: 17 January 2013 – Published: 31 January 2013

Correspondence to: W. J. Dong (dongwj@bnu.edu.cn) and
W. P. Yuan (wenpingyuancn@yahoo.com)

Published by Copernicus Publications on behalf of the European Geosciences Union.

Title Page
Abstract Introduction
Conclusions References
Tables Figures
◀| |▶
◀ ▶
Back Close
Full Screen / Esc
Printer-friendly Version
Interactive Discussion

Abstract

Drought has been a concern of global and regional water, carbon and energy cycles. From 1999 to 2011, North China experienced a multiyear precipitation reduction, which decreased significantly water availability as indicated by decreased soil moisture and Palmer Drought Severity Index. In this study, three light use efficiency models (CASA, MODIS-GPP and EC-LUE) and one dynamic vegetation model (IBIS) were used to characterize the impacts of long-term drought on terrestrial carbon fluxes over the North China. All of four models showed the reduction in averaged GPP of 0.026–0.047 $\mathrm{Pg\,C\,yr^{-1}}$ from 1999 to 2011 compared to 1982–2011. Based on IBIS model, simulated ecosystem respiration fell from 1999 to 2011 by 0.016 $\mathrm{Pg\,C\,yr^{-1}}$. Multiple precipitation reduction changed the regional carbon uptake of 0.0014 $\mathrm{Pg\,C\,yr^{-1}}$ from 1982 to 1998 to a net source of 0.018 $\mathrm{Pg\,C\,yr^{-1}}$. Moreover, a pronounced decrease of maize yield was found ranging from 1999 to 2011 versus the average of 1978–2011 at almost all provinces over the study region. The largest reduction of maize yield occurred in the Beijing (2499 $\mathrm{kg\,ha^{-1}\,yr^{-1}}$), Jilin (2180 $\mathrm{kg\,ha^{-1}\,yr^{-1}}$), Tianjing (1923 $\mathrm{kg\,ha^{-1}\,yr^{-1}}$) and Heilongjiang (1791 $\mathrm{kg\,ha^{-1}\,yr^{-1}}$), and maize yield anomaly was significantly correlated with the precipitation through May and September over the entire study area. Our results revealed that recent climate change, and especially drought-induced water stress, is the dominant cause of the reduction in the terrestrial carbon sink.

1 Introduction

As one of the major issues in global environmental changes, drought has attracted widespread attention from both scientists and policy-makers in the past few decades (IPCC, 2007). Global total of very dry land areas has increased from 12 % to 30 % since 1972 indicated by Palmer Drought Severity Index (Dai et al., 2004). Recent large-scale and severe droughts have occurred in Europe in 2003 (Ciais et al., 2005), western North America from 1999 to 2004 (Cook et al., 2004), and the Sahel region of Africa from the 1960s to present (Dai et al., 2004). Analyzing prediction data from the IPCC AR4 multimodel ensemble-mean under the SRES A1B scenario, soil moisture was found general drying over most of the global land and warned a world-wide drought by the late 21st century (IPCC, 2007). Given the strong coupling between carbon and hydrologic cycles, such drying may have significant impacts on terrestrial carbon dynamics and atmospheric carbon dioxide concentrations and lead to a positive feedback to the global climate system.

Several of studies have reported the impacts of drought on ecosystem carbon budget. An extreme drought in Europe during 2003, for example, not only led to a crop shortfall (more than 20 %) in Southern Europe, but also caused about 0.5 Pg of carbon to be lost from terrestrial ecosystems, which corresponds to four years of net ecosystem carbon sequestration (Ciais et al., 2005). A drying trend in the Southern Hemisphere has decreased NPP during the past decade (2000 to 2009) in that area, resulting to a reduction in the global NPP of 0.55 Pg of carbon (Zhao et al., 2010). Over Canada's boreal forests, tree mortality rates increased by an overall average of 4.7 % yr^{-1} from 1963 to 2008, and drought-induced water stress is the dominant cause of the observed increases in tree mortality rates (Peng et al., 2011). Western Canada's boreal forests may become net carbon sources if the climate change–induced droughts continue to intensify (Ma et al., 2012). Over western North American, terrestrial ecosystem carbon sink declined by 51 % during the 2000–2004 droughts with a reduction in river discharge and a loss of cropland productivity (Schwalm et al., 2012).

North China has experienced frequent severe droughts during the second half of twentieth century (Wang et al., 2003; Zou et al., 2005). Studies based on climate station data showed that much of North China has experienced droughts since the 1950s, with the most severe and prolonged droughts having occurred since 1990 (Zhai et al., 2010). Moreover, drought variations displayed multiple time scales and seasonal differences (Wang et al., 2003). An analysis based on the Palmer Drought Severity Index (PDSI) found that almost every year had more than 25 % of the county under drought threat over North China from the period 1951–2003 (Zou et al., 2005). For instance, the

2008/09 winter drought in Northeastern China was one of the worst in the past 50 yr, resulting in an estimated 2.3 billion U.S. dollars in economic losses and subjecting more than 10 million people to water shortages (Gao et al., 2009).

However, there are a limited number of studies on the effects of drought on ecosystem carbon occurring over the North China. The overarching goal of this study is to conduct the assessment of the impacts of severe extended droughts on the carbon balance of terrestrial ecosystems in North China. Specific objectives are to (1) evaluate spatial and temporal distributions of annual precipitation changes across the North China over the long-term period; and (2) investigate the magnitude and mechanism on the impacts of drought on carbon budget of terrestrial ecosystems.

2 Data and method

2.1 Study area and data

The study area for this research encompasses 11 provinces of North China (Fig. 1), which covers approximately 2.90 million km^2 and accounts for 37 % of the territory of the China. The study area is predominantly composed of various temperature forests, grasslands, croplands and deserts, including 41 % area of forest, 36 % grassland and 57 % cropland of the whole China, and it is one of the most important carbon budget and crop production areas of China.

Meteorology data were obtained from the National Climate Center of China Meteorological Administration, and locations of the stations can be referred to Fig. 1. Daily meteorology data from 185 stations spanning 1960–2011 were analyzed. Thin plate smoothing splines method was used to generate daily mean air temperature ($\mathrm{T_m}$), relative humidity (R_h), precipitation (Prec), wind speed (W_s) and sun shine hours (S_h) for all of China at a spatial resolution of 25 km of latitude and longitude for the period 1960–2011. The fitted trivariate splines incorporated a spatially varying dependence on ground elevation and were able to adapt automatically to the large variation in station density over China. A comprehensive introduction to the technique of thin plate smoothing splines, with various extensions, is given in Wahba (1990). Moreover, a simple method was used to calculate downward solar radiation (R_g) from sun shine hours data, and R_g was transferred to photosynthetically active radiation (PAR) with the ratio of 0.5.

The soil moisture data for five different layers (0–10, 10–20, 20–30, 30–40, 40–50 cm) with a 10 day interval were obtained from the National Meteorological Information Center of the China Meteorological Administration. Because the primary objective of this paper is to study the effects of precipitation on soil moisture, we excluded irrigation stations. Annual mean soil moisture was estimated on the basis of the average of soil moisture data for each 10 day interval during the May to September. For each year at each site, if the missing data was more than 20 %, we did not consider the corresponding year at this site as available. Moreover, when investigating the long-term change trend of soil moisture, we only consider stations for which at least 80 % years of data are available during the study period.

Palmer Drought Severity Index (PDSI) created by Dai et al. (2004) was used to investigate long-term drought trend over North China. The PDSI is the most prominent index of meteorological drought used worldwide. The PDSI incorporates antecedent and current moisture supply (precipitation) and demand (evapotranspiration) into a hydrological accounting system. It also has been used to quantify long-term changes of drought events over global land in the 20th and 21st century (Dai et al., 2004; Burke et al., 2006).

Moreover, harvest data of maize from province-level statistics from 1982 to 2011 was used to analyze the impacts of drought over the study areas (Ministry of Agriculture, PRC, 2009, 2010, 2011, 2012). Usually, maize is cultivated over the study area without irrigation, therefore, the maize yield can be used to reflect the impact of drought on crop production. Crop yield is influenced by various biotic, abiotic and anthropogenic factors (e.g. environment, management) and will show trends due to improvements in genetics, fertilizer application policies, etc. Crop yield time series were de-trended using the best fit least squares regression method as recommended by Goldblum (2009). After removal of the trend yield, the remaining part can be assumed to reflect the impact of climatic factors.

2.2 Carbon cycle models

In this study, three satellite-based light use efficiency (LUE) models (i.e. CASA, EC-LUE and MODIS-GPP) and one process-based ecosystem model (i.e. IBIS), which have been widely validated and applied at global scales, were selected to examine the impact of drought events on vegetation GPP and carbon uptake over the North China.

CASA is a classic light use efficiency model that utilises satellite measurements to estimate vegetation net primary production (Potter et al., 1993). It directly translates absorbed photosynthetically active radiation (PAR) into vegetation production based on the notion of light use efficiency (LUE), which is a product of optimal efficiency and the regulatory functions of environmental factors (e.g. temperature and water stress). CASA model simulates directly NPP, and an approximate conversion of 0.5 between NPP and GPP is used in this study.

The EC-LUE model is driven by only four variables: the normalised difference vegetation index (NDVI), photosynthetically active radiation (PAR, $\mathrm{MJ\,m^{-2}}$), air temperature (T, °), and the Bowen ratio of sensible to latent heat flux (Yuan et al., 2007, 2010). GPP was computed from the fraction of PAR absorbed by the vegetation canopy (fPAR), PAR, and down-regulators that represent plant stresses due to suboptimal temperature (T_s) and water (W_s).

MODIS-GPP algorithms (Running et al., 1999) rely heavily on the LUE approach, with inputs from MODIS LAI/fPAR (MOD15A2), land cover, and biome-specific climatologic data sources from NASA's Data Assimilation Office. Light use efficiency is calculated based on two factors: the biome-specific maximum conversion efficiency $\varepsilon_{\max}$, a multiplier that reduces the conversion efficiency when cold temperatures limit plant function, and a second multiplier that reduces the maximum conversion efficiency when vapour pressure deficit (VPD) is high enough to inhibit photosynthesis. It is assumed that soil water deficit covaries with VPD and that VPD will account for drought stress.

We use a processes-based terrestrial carbon models: Integrated BIosphere Simulator (IBIS2.6, Foley et al., 1996). IBIS hierarchically organized to allow for explicit coupling among ecological biophysical and physiological processes at different timescales (Foley et al., 1996). IBIS uses a mechanistic Farquhar model for treatment of canopy photosynthesis (Farquhar et al., 1980). The CO_2 production models are established for ecosystem respiration processes on the principle of mass balance of carbon in ecosystems, and which generally share a common structure that partitions carbon input into several pools, from which carbon is released via respiratory processes.

Fifteen EC sites in China, covering various ecosystem types such as forests, grasslands and croplands, and prairies, were included in this study to verify their ability to reproduce the observed GPP, Ecosystem Respiration (TER) and Net Ecosystem Production (NEP) (Fig. 1). Half-hourly or hourly averaged regional radiation (R_a), photosynthetically active radiation (PAR), air temperature (T_a), and friction velocity (u^*) were used with the net ecosystem exchange of CO_2 (NEE) in this study. Data analyses procedures were presented in Yuan et al. (2010), Li et al. (2012) and Zhang et al. (2012). Briefly, daily NEE, TER, and meteorological variables were synthesized based on half-hourly or hourly values. The tower-based GPP was calculated as the result of NEP and TER. Daytime TER is usually developed from nighttime NEE measurements which equals to night respiration, and estimated by using daytime temperature and a linear equation describe the temperature dependence of respiration. The daily values were indicated as missing when missing data was more than 20 % of the entire data on a given day. Otherwise, daily values were calculated by multiplying the averaged hourly rate by 24 h.

Then, we simulated the changes in carbon fluxes from 1982 to 2011 using interpolated climate and satellite-based leaf area index (LAI). AVHRR GIMMS LAI during 1982–2006 and MODIS LAI during 2000–2011 series were used to generate a single, continuous LAI record. A linear regression method was used to combine these two datasets (Zhang et al., 2008).

3 Results

3.1 Climate change over the North China

North China experienced a multiyear precipitation anomaly since 1999 (Fig. 2). Eleven of thirteen years during 1999–2011, exception of 2003 and 2010, showed lower annual mean precipitation over all meteorology stations with decreased range from 3 % to 21 % compared with long-term average during 1960–2011 (Fig. 2). More than 84 % stations over the study area show the decreased annual mean precipitation during 1999–2011, and significant decreased trends were found at 30 % stations (Fig. 3). A general decrease in the precipitation days has been observed over the 89 % stations (Fig. 3), and 4 % decrease of precipitation days during 1999–2011 compared with long-term average (Fig. 2). Seasonal changes in precipitation patterns are also apparent, and precipitation shows the obvious decrease in summer and autumn (Fig. 2). In stark contrast, winter and spring have experienced an increase in precipitation (Fig. 2).

Contrary to decreased precipitation, over the past decade, a strong warming of North China is firmly supported by continuous measurements. Mean annual temperature increases at a rate of 0.258° per decadal years since 1960s (Fig. 2), which is quite higher than 0.074 mean level across the whole world. Stations of 87 % show significant higher temperature from 1999 to 2011 compare with that of past five decades (Fig. 3a). The nine warmest years of ten occurred after 1999. Increases in temperature lead to increases in the moisture-holding capacity of the atmosphere at a rate of about 7 % per °C. The results show significant reduction of relative humidity from 1999 to 2011 (Fig. 3b). A general decrease in the sunshine duration has been observed over the most stations of study region, and the results show 4 % decrease during 1999–2011 compared with long-term average (Fig. 3c). Moreover, through the same study period, a significant reduction of wind speed has also been observed over the North China, and more than 90 % stations show significant lower wind speed (Fig. 3d).

Reduced precipitation and increased temperature also clearly impacted the water balance on the regional scale. During 1999 to 2009, more soil monitor sites showed negative anomaly of annual mean soil moisture compared with the previous 17 yr (i.e. from 1982 to 1998) (Fig. 4). On average, from 1999 to 2009, more than 62 % sites showed decreased soil moisture compared with long-term mean values. Regional average precipitation explained very well the increased number of soil monitor sites with negative anomaly of soil moisture (Fig. 4). Moreover, 89 soil monitor sites which had more than 80 % measurements to investigate the decreased magnitude. The results showed decreased soil moisture over the study period compared with the baseline period at 67 % sites (Fig. 5a).

The PDSI has been proven to be the most effective index for determining long-term meteorological drought, which has been used to identify the severity of droughts over the North China. A Palmer Drought Severity Index (PDSI) at 2.5° resolution was used as a surrogate of soil moisture to measure environmental water stress by combining information from both evaporation and precipitation. A lower PDSI generally implies a drier climate. The differences of the annual PDSI between two periods of 1999–2011 and 1960–2011 are shown in Fig. 5. Increased drought indicated by PDSI has occurred over the North China (Fig. 5b).

3.2 Impacts of decreased precipitation on carbon cycle

Estimated GPP from EC measurements at 15 sites were used to validate the EC-LUE, CASA and MODIS-GPP product. Three models successfully predicted the magnitudes and seasonal variations of GPP. CASA, EC-LUE and MODIS-GPP explained about 59 %, 80 % and 75 % of the variation of monthly GPP at all sites, respectively (Fig. 6a–c). We next validated IBIS on the performance of GPP, ecosystem respiration (TER) and NEE. The results showed relative consistence between observations and simulations for three variables (Fig. 6d–f).

Although there are still large differences of simulated GPP among these four models, the interannual variability of GPP with precipitation anomaly shows relatively consistent changes (Fig. 7). The results show a pronounced GPP decrease ranging from 1999 to 2011 versus the average of 1982–2011 at almost all provinces over the study region (data not shown). For the entire study region, simulations showed the obvious reduction in averaged GPP from 1999 to 2011 compared to 1982–2011 with the decreased magnitude by 0.046 $\mathrm{Pg\,C\,yr^{-1}}$, 0.026 $\mathrm{Pg\,C\,yr^{-1}}$, 0.047 $\mathrm{Pg\,C\,yr^{-1}}$ and 0.026 $\mathrm{Pg\,C\,yr^{-1}}$ for EC-LUE, CASA, MODIS and IBIS model respectively (Fig. 7). Similar spatial patterns of GPP anomaly were found among the four models (Fig. 8). Only at the northern, southern and western regions of study area, increased GPP was found, and other most regions showed decreased GPP trends. Simulated respiration (TER) fell over China from 1999 to 2011 by 0.016 $\mathrm{Pg\,C\,yr^{-1}}$, tailing off with a larger GPP reduction of 34 to 59 % (Fig. 7). The parallel reduction in GPP and TER over China equates to an anomalous source from 1999 to 2011 to the atmosphere of 0.018 $\mathrm{Pg\,C\,yr^{-1}}$, and multiple precipitation reduction changed the regional carbon uptake of 0.0014 $\mathrm{Pg\,C\,yr^{-1}}$ from 1982 to 1998 to a net source.

Similarly, maize yield also decreased significantly after 1999. On average, maize yield from 1999 to 2011 was below by 440 $\mathrm{kg\,ha^{-1}\,yr^{-1}}$ compared with linear trend yields. The largest reduction of crop yield was found in the Beijing (2499 $\mathrm{kg\,ha^{-1}\,yr^{-1}}$), Jilin (2180 $\mathrm{kg\,ha^{-1}\,yr^{-1}}$), Tianjing (1923 $\mathrm{kg\,ha^{-1}\,yr^{-1}}$) and Heilongjiang (1791 $\mathrm{kg\,ha^{-1}\,yr^{-1}}$). Corn yield anomaly was significantly correlated with the precipitation through May and September over the entire study area during 1982–2011, indicating the dominant role of water limitations (Fig. 9).

4 Discussion

Terrestrial ecosystems have been experiencing frequent extreme drought events, which have already exerted profound impacts on global economy, food security and terrestrial ecosystems (Ciais et al., 2005). Studies on the effects of drought on ecosystem carbon fluxes have been conducted based on short-term/seasonal observations, however, there are a limited number of studies on the effects of long-term severe drought on ecosystem carbon dynamics (Krishnan et al., 2006).

Several very severe drought events have hit China in the 1960s, in the late 1970s and early 1980s, and in the late 1990s (Zhai et al., 2010). In this study, the results showed decadal-scale precipitation reduction since 1999 over the North China. Other lines of evidence also support our result that precipitation shows a decreasing trend at the study region. Analysis based on 355 rain gauge stations showed no significant long-term trend in country-average precipitation since 1960, however, the drier regions of Northeastern China (including North China and Northeast China) are receiving less and less precipitation in summer and autumn with 12 % decline since 1960 (Piao et al., 2010). Reconstructed precipitation data of the past 232 yr based on tree-rings records do not indicate any apparent long-term decreasing or increasing trend of precipitation over the North China during the latest 100 yr, however, a strong decreasing trend was found over the most recent decade (Chen et al., 2011). Results from climate models under the IPCC A1B scenario show that the recently observed drier Northeast China may further intensify (Wang et al., 2005).

China is located in the East Asian monsoon region, which is highly vulnerable to any anomalous monsoon rainfall, yielding droughts or floods. In general, strong summer monsoon results in flood in the Northern China, whereas droughts can occur during the years with weak summer monsoon in the most part of Eastern China, especially in the North China (Guo, 1994). Previous study showed the weakening summer monsoon during the recent years (Ding et al., 2008). Moreover, recent studies demonstrate that a weakening in surface sensible heating over the Tibetan Plateau results in a weaker equilibrated Sverdrup balance between positive vorticity generation and latent heat release (Liu et al., 2012). Consequently, the convergence of water vapor transport is confined to South China, forming a unique anomaly pattern in monsoon rainfall, named “south wet and north dry.” Therefore, recent decreased precipitation trends are expected from the probable weakening of the summer monsoon.

Continuous multiyear precipitation deficit of has resulted to substantially decreased trend of available water within the terrestrial ecosystems. Our results showed soil moisture sites with drier trends were more than those with wetter trends (Fig. 5). Other lines of evidence also support our conclusions that soil moisture and river runoff at the study region have showed a significant reduction trends (Han et al., 2009; Li et al., 2010, 2011). For example, based on the observed soil moisture at 16 sites over the Northeast China, it was found that the surface soil humidity during crop growth period in 1980–2005 had a decreasing trend, and tended to be drier, especially in the west and south region of the Northeast China (Jiang et al., 2009).

Severe extended droughts during the twentieth century had significant impacts on terrestrial carbon cycling, suggesting that severe extended droughts should be considered in regional carbon budget studies. The magnitude of the terrestrial carbon sink could be substantially overestimated without considering extreme climate events. Our estimates suggested a reduction in the regional GPP of 0.026 to 0.047 $\mathrm{Pg\,C\,yr^{-1}}$. Large-scale droughts have reduced regional GPP, counteracting the positive impacts of increased temperature and enlarged growing season. Based on the observations and models, previous of studies also showed impacts of drought on vegetation production across the various geographical and climate regions from regional to continental scales (Zhao et al., 2010; Schwalm et al., 2012). In this study, there were not long-term ecosystem carbon flux observations, so we used three satellite-based models and one dynamic model for investigating the impacts of drought in order to reduce the uncertainties of individual model. Water indexes were diverse among the models, and there were large differences on the spatial pattern of water stress changes during the study period (Fig. 9). However, all of four models demonstrated the substantial reductions of water availability. As the result, there were highly consistent interannual variations and decreased GPP trends from 1999 to 2011 derived from all models. It should be notice that there were large differences of magnitude and spatial patterns of decreased GPP among the four models, which implied that we need to understand better the link of water shortage and carbon cycle processes, and improve the abilities of ecosystem models to simulate the impacts of drought.

During the study period, ecosystem respiration fell in parallel with GPP at most regions (Fig. 8). Drought can result into the reduction in both plant respiration (due to diminished substrates) and microbial soil respiration (also due to drought). Low water availability decreased ecosystem production to supply carbon substrate and decomposition (Gärdenäs et al., 2000). Moreover, extreme dry conditions induce dormancy or spore formation in soil microorganisms and/or cell dehydration (Stark and Firestone, 1995). At low moisture content, bacteria maintain only a basic metabolism as in dormancy. Dormancy can result in substantial reductions in respiration per unit of biomass or reductions in total respiratory biomass (Luo et al., 2006).

Northeast China, including the Heilongjiang, Jilin, Liaoning, Hebei provinces is one of the most important grain producing areas of China. Corn acreage in this region accounts for 26.3 % of the corn area in the country and accounts for about 29.4 % of Chinese total corn grain production and thus plays a significant role in ensuring Chinese food security. Knowledge of the potential effects of climate change on corn production in Northeast China will be highly valuable, not only for China but also for the world (Sternberg, 2012). Although recent studies showed that climate change would increase corn yield in North China (IPCC, 2007), Zhang et al. (2010) reported opposite results indicating that average yields may decrease about 2–3 % if no countermeasures would be taken. These contradictory conclusions may be attributed by the impact of drought events.

5 Summary

Fossil fuel emissions aside, North China is an important sink of carbon dioxide at present. Year-to-year variations in this carbon sink are linked to variations in hydroclimate that affect net ecosystem productivity. This study attempts to quantify the long-term consequences of extreme climate conditions on carbon cycles compared with other studies focusing on short-term impact. Our results showed that continuous multi-year precipitation reduces have the potential to significantly alter long-term ecosystem water balances and carbon budgets. The area-integrated strength of the North China carbon sink declined by 0.011 $\mathrm{Pg\,C\,yr^{-1}}$ during the 1999–2011 drought. We further document a pronounced drying of the terrestrial biosphere during this period, together with a reduction in soil moisture and a loss of cropland productivity. In China, more frequent extreme drought events may counteract the effects of the anticipated mean warming and lengthening of the growing season, and erode the productivity of ecosystems, reversing sinks to sources, and contributing to positive carbon-climate feedbacks.

Acknowledgements. This study was supported by the National Basic Research Program of China (2010CB833504 and 2010CB950504), the National Natural Science Foundation of China (40830957) and the Fundamental Research Funds for the Central Universities. We thank the Coordinated Observations and Integrated Research over Arid and Semi-arid China (COIRAS) and Chinese Terrestrial Ecosystem Flux Research Network (ChinaFlux) for providing the eddy covariance flux data.

References

Burke, E. J., Brown, S. J., and Christidis, N.: Modeling the recent evolution of global drought and projections for the twenty-first century with the Hadley centre climate model, J. Hydrometeorol., 7, 1113–1125, 2006.

Chen, Z. J., He, X. Y., Cook, E. R., He, H. S., Chen, W., Sun, Y., and Cui, M. X.: Detecting dryness and wetness signals from tree-rings in Shenyang, Northeast China, Palaeogeogr. Palaeocl., 302, 301–310, 2011.

Ciais, P., Reichstein, M., Viovy, N., Granier, A., Ogée, J., Allard, V., Aubinet, M., Buchmann, N., Bernhofer, C., Carrara, A., Chevallier, F., Noblet, N. D., Friend, A. D., Friedlingstein, P., Grünwald, T., Heinesch, B., Keronen, P., Miglietta, F., Ourcival, J. M., Papale, D., Pilegaard, K., Rambal, S., Seufert, G., Soussana, J. F., Sanz, M. J., Schulze, E. D., Vesala, T., and Valentini, R: Europe-wide reduction in primary productivity caused by the heat and drought in 2003, Nature, 437, 529–533, 2005.

Cook, E. R., Woodhouse, C. A., Eakin, C. M., Meko, D. M., and Stahle, D. W.: Long-term aridity changes in the western United States, Science, 306, 1015–1018, 2004.

Dai, A., Trenberth, K. E., and Qian, T. A.: Global data set of Palmer Drought Severity Index for 1870–2002: relationship with soil moisture and effects of surface warming, J. Hydrometerol., 5, 1117–1130, 2004.

Ding, Y. H., Wang, Z. Y., and Sun, Y.: Inter-decadal variation of the summer precipitation in East China and its association with decreasing Asian summer monsoon. Part I: Observed evidence, Int. J. Climatol., 28, 1139–1161, 2008.

Foley, J. A., Prentice, I. C., Ramankutty, N., Levis, S., Pollard, D., Sitch, S., and Haxeltine, A.: An integrated biosphere model of land surface processes, terrestrial carbon balance, and vegetation dynamics, Global Biogeochem. Cy., 10, 603–628, 1996.

Farquhar, G. D., Caemmerer, S., and Berry, J. A.: A biogeochemical model of photosynthetic CO_2 assimilation in leaves of C3 species, Planta, 149, 78–90, 1980.

Gao, H. and Yang, S.: A severe drought event in northern China in winter 2008–2009 and the possible influences of La Niña and Tibetan Plateau, J. Geophys. Res., 114, D24104, doi:10.1029/2009JD012430, 2009.

Gärdenäs, A. I.: Soil respiration fluxes measured along a hydrological gradient in a Norway spruce stand in south Sweden, Plant Soil, 221, 273–280, 2000.

Goldblum, D.: Sensitivity of corn and soybean yield in Illinois to air temperature and precipitation: the potential impact of future climate change, Phys. Geogr., 30, 27–42, 2009.

Guo, Q.: Monsoon and droughts/floods in China, in: Asian Monsoon, edited by: Ding, Y., China Meteorology Press, Beijing, China, 65–75, 1994.

Han, J. J., Gao, Y. G., Nan, R., and Cao, W. D.: Characteristics of soil moisture variation in main agricultural areas of Heilongjiang Province from 1984 to 2005, Chin. J. Agrometeorol., 30, 41–44, 2009 (in Chinese with English Abstract).

IPCC: Climate change 2007: The Physical Science Basis, Contribution of Working Group I to the Fourth Assessment Report of the Intergovernmental Panel on Climate Change, Cambridge University Press, Cambridge, UK and New York, NY, USA, 241–254, 2007.

Jiang, L. X., Li, S., Ji, Y. H., Zhu, H. X., Yan, P., Wang, P., Wang, C. Y., and Han, J. J.: Responses of soil humidity on Songnen Plain to climate change in 1980–2005, Chin. J. Appl. Ecol., 20, 91–97, 2009 (in Chinese with English Abstract).

Krishnan, P., Black, T. A., Grant, N. J., Barr, A. G., Hogg, E. H., Jassal, R. S., and Morgenstern, K.: Impact of changing soil moisture distribution on net ecosystem productivity of a boreal aspen forest during and following drought, Agr. Forest Meteorol., 139, 208–223, 2006.

Li, M. X., Ma, Z. G., and Du, J. W.: Trend analysis of soil moisture over the Shanxi Province of China, Sci. China Earth Sci., 40, 363–379, 2010 (in Chinese with English abstract).

Li, M. X., Ma, Z. G., and Niu, G. Y.: Spatial and temporal patterns of simulation of soil moisture over the China, Chinese Sci. Bull., 56, 1288–1300, 2011 (in Chinese with English abstract).

Li, X. L., Liang, S. L., Yuan, W. P., Yu, G. R., Cheng, X., Chen, Y., Zhao, T. B., Feng, J. M., Ma, Z. G., Ma, M. G., Liu, S. M., Chen, J. Q., Shao, C. L., Li, S. G., Zhang, X. D., Zhang, Z. Q., Sun, G., Chen, S. P., Ohta, T., Varlagin, A., Miyata, A., Takagi, K., Saiqusa, N., and Kato, T.: Estimation of evapotranspiration over the terrestrial ecosystems in China, Ecohydrology, doi:10.1002/eco.1341, 2012.

Liu, Y. M., Wu, G. X., Hong, J. L., Dong, B. W., Duan, A. M., Bao, Q., and Zhou, L. J.: Revisiting Asian monsoon formation and change associated with Tibetan Plateau forcing: II. Change, Clim. Dynam., 39, 1183–1195, 2012.

Luo, Y. Q. and Zhou, X. H.: Soil Respiration and the Environment, Academic Press, Burlington, USA, 2006.

Ma, Z. H., Peng, C. H., Zhu, Q., Chen, H., Yu, G. R., Li, W. Z., Zhou, X. L., Wang, W. F., and Zhang, W. H.: Regional drought-induced reduction in the biomass carbon sink of Canada's boreal forests, P. Natl. Acad. Sci. USA, 109, 2423–2427, 2012.

Ministry of Agriculture, PRC.: China Agriculture Statistics Report, China Agriculture Press, China, 2009.

Ministry of Agriculture, PRC.: China Agriculture Yearbook 2009, China Agriculture Press, Beijing, China, 2010.

Ministry of Agriculture, PRC.: China Agriculture Yearbook 2010, China Agriculture Press, Beijing, China, 2011.

Ministry of Agriculture, PRC.: China Agriculture Yearbook 2011, China Agriculture Press, Beijing, China, 2012.

Peng, C. H., Ma, Z. H., Lei, X. D., Zhu, Q., Chen, H., Wang, W. F., Liu, S. R., Li, W. Z., Fang, X. Q., and Zhou, X. L.: A drought-induced pervasive increase in tree mortality across Canada's boreal forests, Nat. Clim. Change, 1, 467–471, 2011.

Piao, S. L., Ciais, P., Huang, Y., Shen, Z. H., Peng, S. S., Li, J. S., Zhou, L. P., Liu, H. Y., Ma, Y. C., Ding, Y. H., Friedlingstein, P., Liu, C. Z., Tan, K., Yu, Y. Q., Zhang, T. Y., and Fang, J. Y.: The impacts of climate change on water resources and agriculture in China, Nature, 467, 43–51, 2010.

Potter, C. S., Randerson, J. T., Field, C. B., Matson, P. A., Vitousek, P. M., Mooney, H. A., and Klooster, S. A.: Terrestrial ecosystem production: a process model based on global satellite and surface data, Global Biogeochem. Cy., 7, 811–841, 1993.

Running, S. W., Nemani, R., Glassy, J. M., and Thornton, P. E.: MODIS daily photosynthesis (PSN) and annual net primary production (NPP) product (MOD17), algorithm theoretical basis document, version 3.0., available at: http://modis.gsfc.nasa.gov/data/atbd/atbd_mod16.pdf, 1999.

Schwalm, C. P., Williams, C. A., Schaefer, K., Baldocchi, B., Black, T. A., Goldstein, A. H., Law, B. E., Oechel, W. C., Paw, U. K. T., and Scott, R. L.: Reduction in carbon uptake during turn of the century drought in western North America, Nat. Geosci., 5, 551–556, 2012.

Stark, J. M. and Firestone, M. K.: Mechanisms for soil moisture effects on activity of nitrifying bacteria, Appl. Environ. Microb., 61, 218–221, 1995.

Sternberg, T.: Chinese drought, bread and the Arab Spring, Appl. Geogr., 34, 519–524, 2012.

Wahba, G.: Spline Models for Observational Data, CBMS-NSF Regional Conference Series in Applied Mathematics 59, SIAM, Philadelphia, Pennsylvania, 1990.

Wang, G. L.: Agricultural drought in a future climate: results from 15 global climate models participating in the IPCC 4th Assessment, Clim. Dynam., 25, 739–753, 2005.

Wang, Z. W. and Zhai, P. M.: Climate change in drought over northern China during 1950–2000, Acta Geogr. Sin., 58, supplement, 61–68, 2003.

Yuan, W. P., Liu, S. G., Zhou, G. S., Zhou, G. Y., Tieszen, L. L., Baldocchi, D., Bernhofer, C., Gholz, H., Goldstein, A. H., Goulden, M. L., Hollinger, D. Y., Hu, Y. M., Law, B. E., Stoy, P. C., Vesala, T., and Wofsy, S. C.: Deriving a light use efficiency model from eddy covariance flux data for predicting daily gross primary production across biomes, Agr. Forest Meteorol., 143, 189–207, 2007.

Yuan, W. P., Liu, S. G., Yu, G. R., Bonnefond, J. M., Chen, J. Q., Davis, K., Desai, A. R., Goldstein, A. H., Gianelle, D., Rossi, F., Suyker, A. E., and Verma, S. B.: Global estimates of evapotranspiration and gross primary production based on MODIS and global meteorology data, Remote Sens. Environ., 114, 1416–1431, 2010.

Zhai, J. Q., Su, B. D., and Krysanova, V.: Spatial variation and trends in PDSI and SPI indices and their relation to streamflow in 10 large regions of China, J. Climate, 23, 649–663, 2010.

Zhang, K., Kimball, J. S., Hogg, E. H., Zhao, M., Oechel, W. C., Cassano, J. J., and Running, S. W.: Satellite-based model detection of recent climate-driven changes in northern high-latitude vegetation productivity, J. Geophys. Res., 113, G03033, doi:10.1029/2007JG000621, 2008.

Zhang, Q., Zeng, J., and Zhang, L. Y.: Characteristics of land surface thermal-hydrologic processes for different regions over North China during prevailing summer monsoon period, Sci. China Earth Sci., 55, 1872–1880, 2012.

Zhang, T. Y., Zhu, J., and Wassmann, R.: Responses of rice yields to recent climate change in China: an empirical assessment based on long-term observations at different spatial scales (1981–2005), Agr. Forest Meteorol., 150, 1128–1137, 2010.

Zhao, M. S. and Running, S. W.: Drought-induced reduction in global terrestrial net primary production from 2000 through 2009, Science, 329, 940–943, 2010.

Zou, X. K., Zhai, P. M., and Zhang, Q.: Variations in droughts over China: 1951–2003, Geophys. Res. Lett., 32, L04707, doi:10.1029/2004GL021853, 2005.

Title Page
Abstract | Introduction
Conclusions | References
Tables | Figures
◀| |▶
◀ ▶
Back | Close
Full Screen / Esc
Printer-friendly Version
Interactive Discussion

Table 1. Name, location, vegetation type and available years of the study sites used for the model validation.

Site name	Latitude, longitude	Vegetation type	Available years
Arou	38.04° N, 100.46° W	Grassland	2008–2009
Changbaishan	42.40° N, 127.09° W	Forest	2002–2008
Changwu	35.20° N, 107.67° W	Grassland	2008–2009
Dongsu	44.09° N, 113.57° W	Grassland	2008–2009
Duolun	42.04° N, 116.29° W	Grassland	2009–2010
Haibei	37.5° N, 101.02° W	Grassland	2008–2009
Miyun	40.63° N, 117.32° W	Cropland	2008–2009
Qingyang	35.59° N, 107.54° W	Grassland	2009
SiziwangFence	41.23° N, 111.57° W	Grassland	2010
SiziwangGraze	41.28° N, 111.68° W	Grassland	2010
Tongyu	44.57° N, 122.88° W	Grassland	2008–2009
Xilinhaote	44.13° N, 116.31° W	Grassland	2006
Yingke	38.86° N, 100.41° W	Cropland	2008–2009
Yuzhong	35.95° N, 104.13° W	Cropland	2008–2009
Zhangye	39.09° N, 100.30° W	Grassland	2008

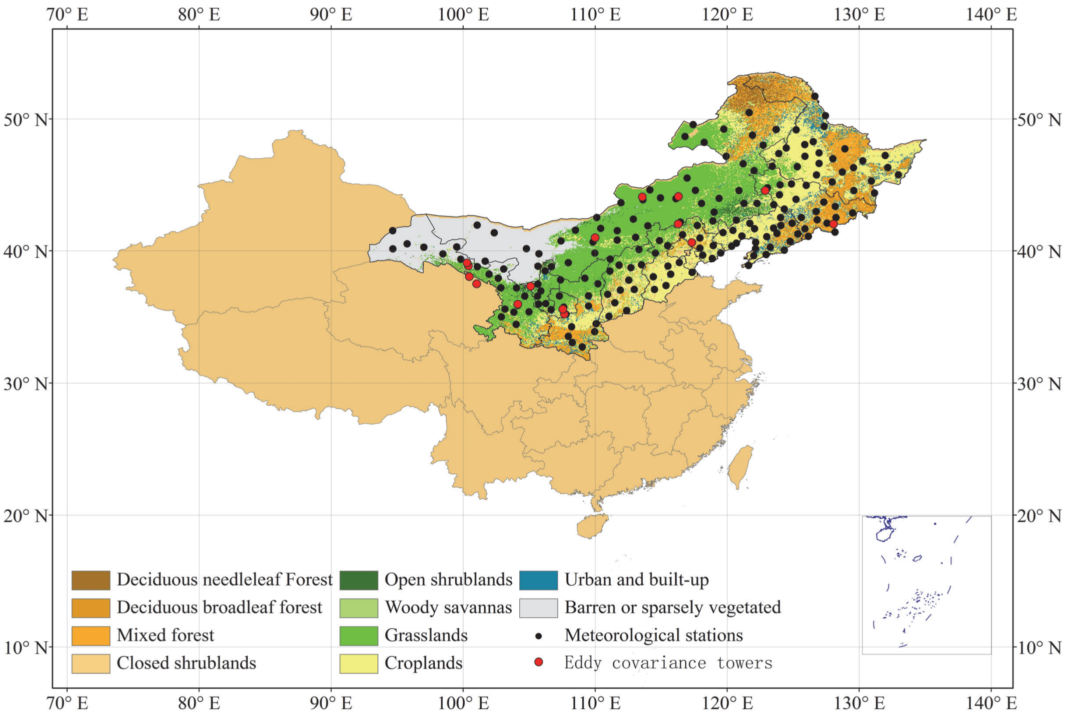

Fig. 1. Spatial domain of the study area, vegetation distribution, meteorological stations and eddy covariance towers location.

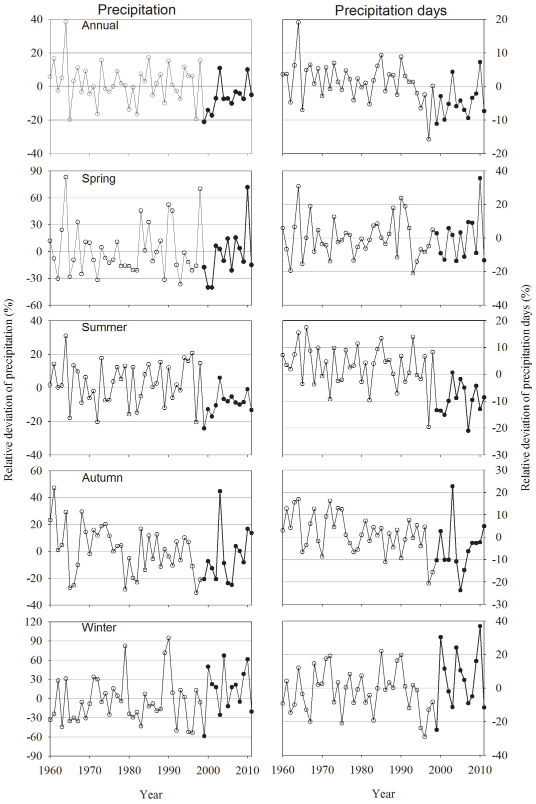

Fig. 2. Observed trends of annual precipitation (left sides) and precipitation days (right sides) in Northern China from 1960 to 2011. The panels show the mean values of entire year, spring, summer, autumn and winter from the top to bottom. The solid dots show the study period of 1999 to 2011.

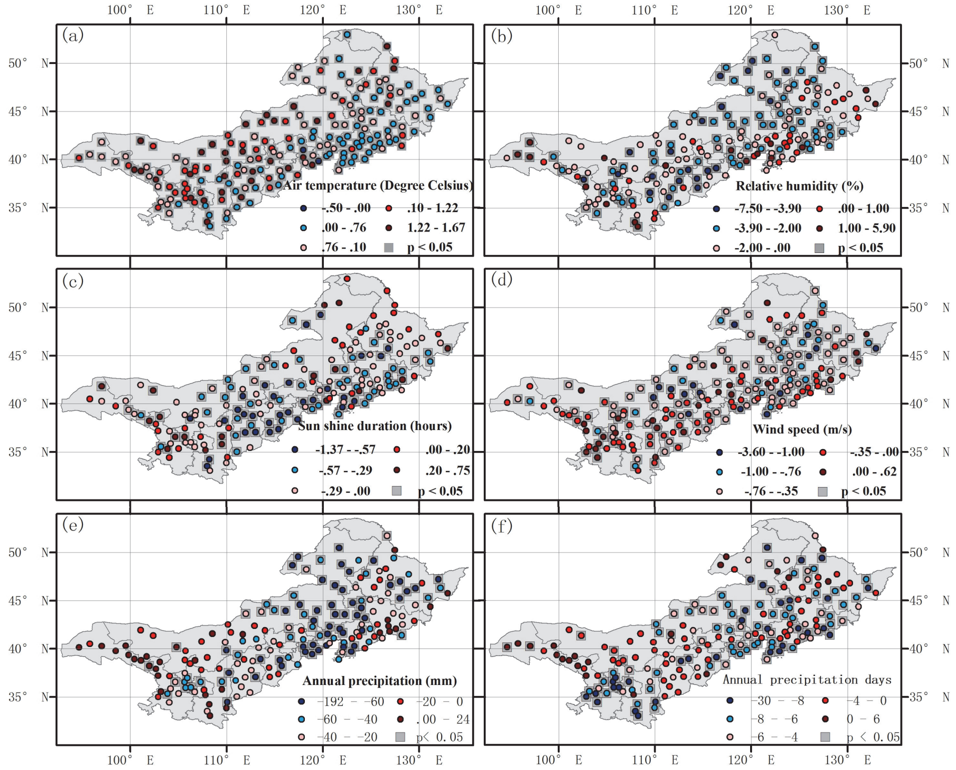

Fig. 3. Observed deviations of mean value during 1999 to 2011 with long term average (1960–2011) in China. **(a)** air temperature, **(b)** relative humidity, **(c)** sun shine duration, **(d)** wind speed, **(e)** annual precipitation and **(f)** precipitation days.

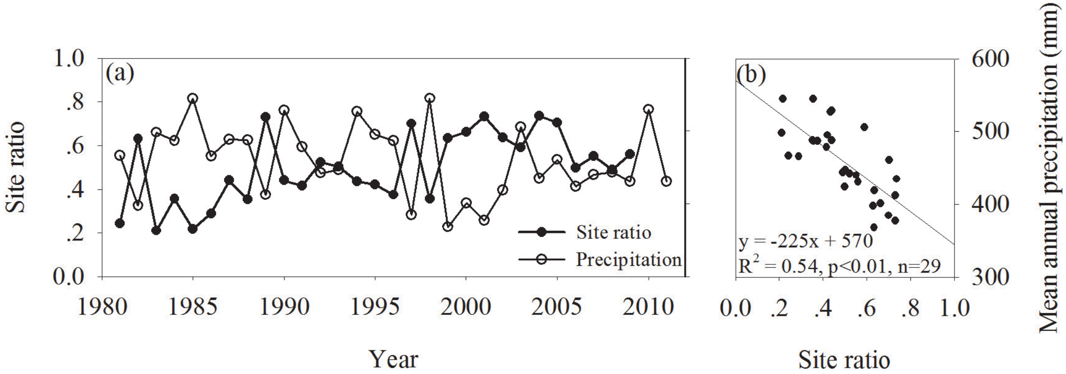

Fig. 4. Changes of soil moisture with precipitation over the North China. **(a)** Interannual variability of soil observation sites friction with negative annual soil moisture (site ratio) and mean annual precipitation; **(b)** the relationship between site ratio with mean annual precipitation.

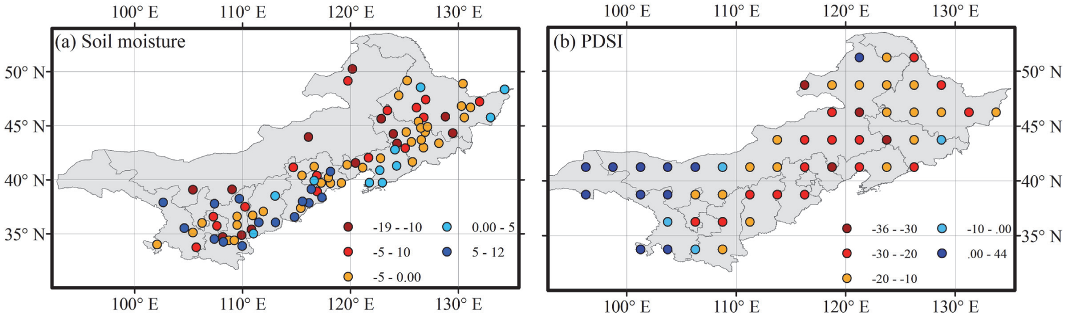

Fig. 5. Difference of soil moisture and PDSI during 1999 to 2011 with long term average (1982–2009 for soil moisture and 1960–2011 for PDSI) over the North China. The values at the figure show the relative percentage.

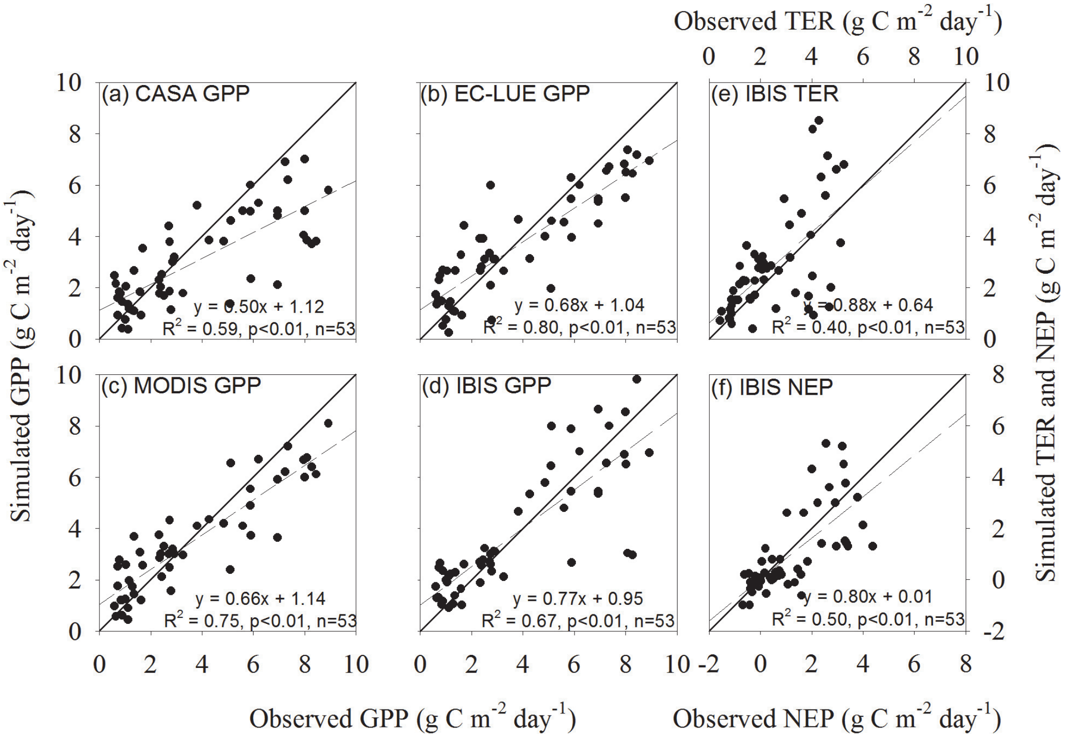

Fig. 6. Observed versus modeled monthly gross primary production (GPP) across 15 eddy covariance towers from **(a)** CASA, **(b)** EC-LUE, **(c)** MODIS-GPP, **(d)** IBIS model; **(e)** TER (ecosystem respiration) and NEP (net ecosystem production) from IBIS model. The solid lines represent the 1 : 1 line.

Title Page
Abstract Introduction
Conclusions References
Tables Figures
◀▮ ▶▮
◀ ▶
Back Close
Full Screen / Esc
Printer-friendly Version
Interactive Discussion

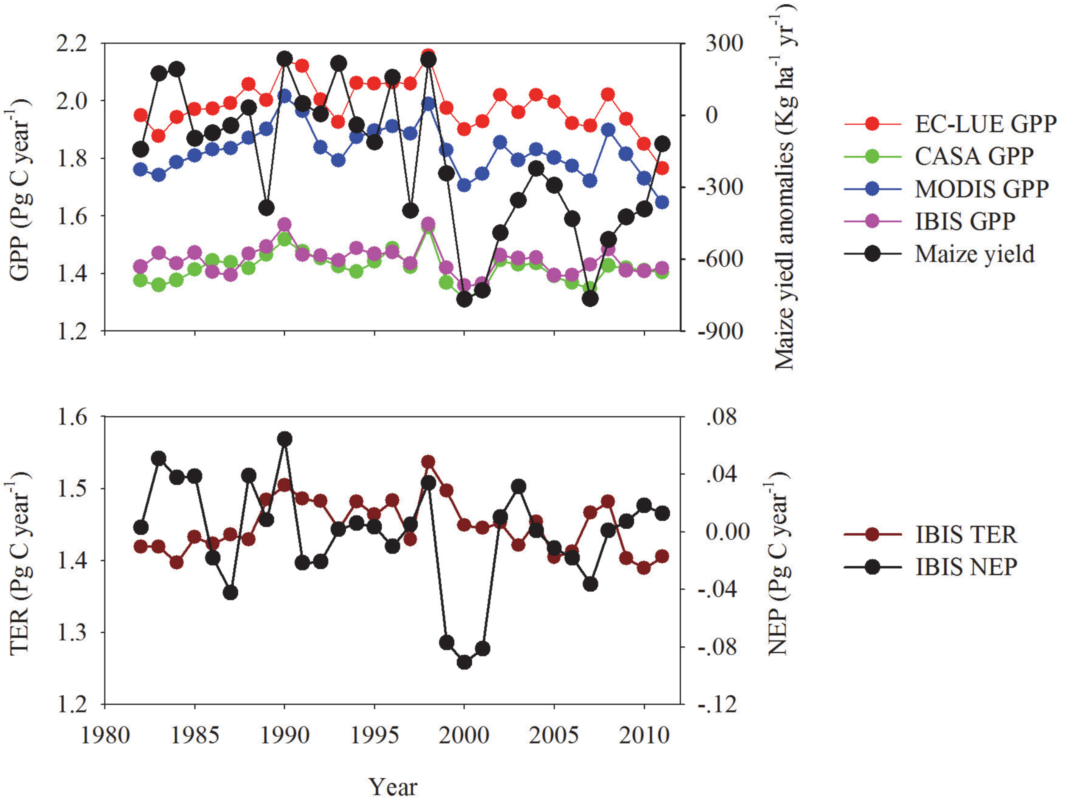

Fig. 7. Regional simulations of GPP, ecosystem respiration (TER), net ecosystem production (NEP) and maize yield anomalies.

Title Page
Abstract | Introduction
Conclusions | References
Tables | Figures
◄| |►
◄ ►
Back | Close
Full Screen / Esc
Printer-friendly Version
Interactive Discussion

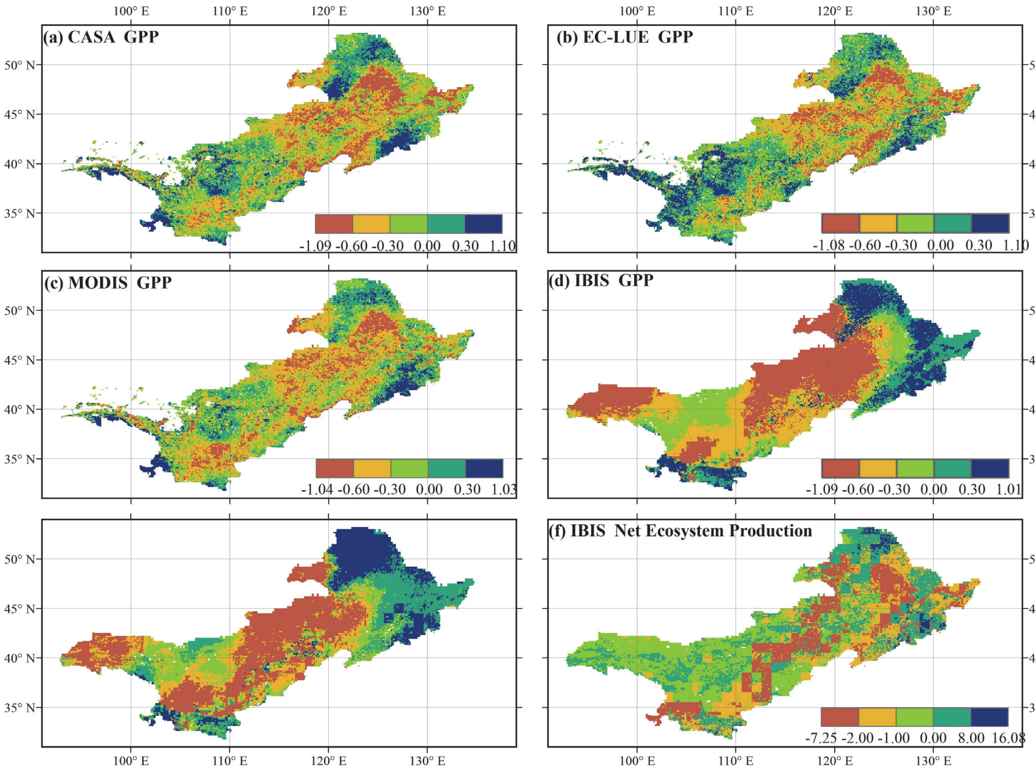

Fig. 8. Spatial patterns of relative deviation of GPP from four models **(a–d)**, TER **(e)** and NEP **(f)** from IBIS.

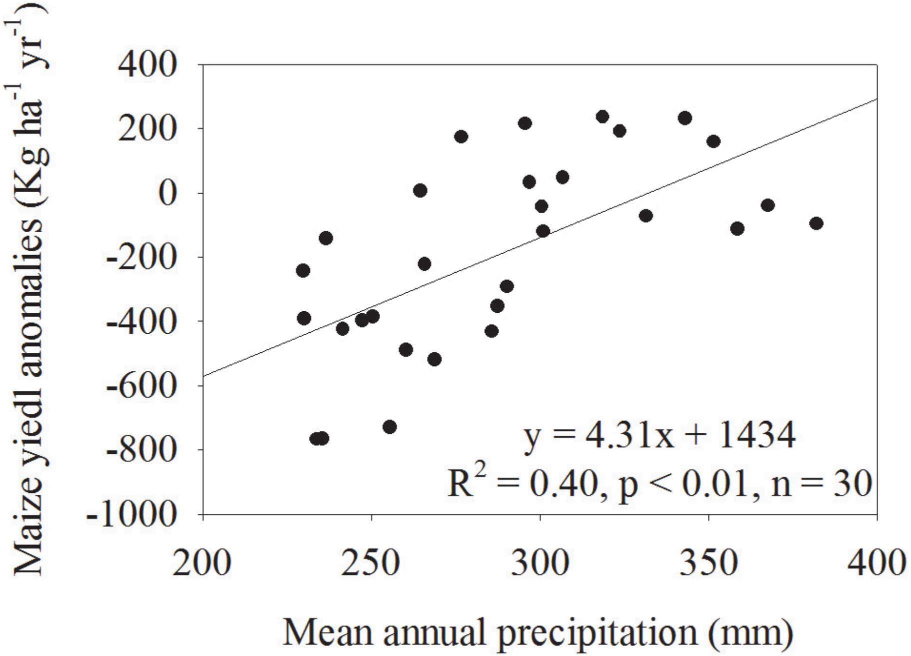

Fig. 9. Relationship between maize yield and mean annual precipitation over the whole study area. To remove the effects of improved agriculture, a linear trend has been generated from the data for indicating the yield trend. The crop yield records show the difference between the observed crop yield and trend value.

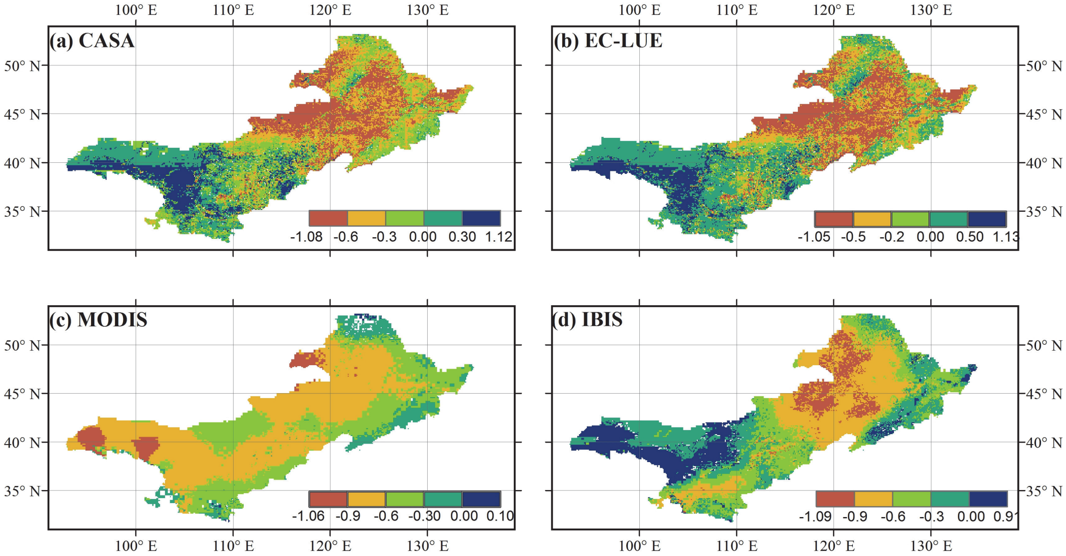

Fig. 10. Spatial patterns of relative deviation of water indexes from four models.